Electr Eng
DOI 10.1007/s00202-017-0639-7

ORIGINAL PAPER

Adaptive direct torque control using Luenberger-sliding mode observer for online stator resistance estimation for five-phase induction motor drives

Hamdi Echeikh[1] · **Ramzi Trabelsi**[2] · **Atif Iqbal**[3] · **Mohamed Faouzi Mimouni**[1]

Received: 21 February 2017 / Accepted: 21 August 2017

Abstract Direct torque control is considered as one of the variable structure control techniques which are characterized by fast response, simplicity and provide direct control of both electromagnetic torque and stator flux by adequate selection of the inverter switches in each sampling period. In case of multiphase motor drives, the increase in voltage vectors offers flexibility to optimize the selection of the inverter switching states, thereby achieving more precise control of the torque and flux. Nevertheless, the criterion for the selection of the inverter states becomes more complex. This aspect is not considered an issue in the traditional three-phase motor drives but needs to be considered in designing the switching table of the direct torque control of five-phase induction motor. Due to the auxiliary vector plane, the low-frequency harmonics need to be eliminated and full utilization of the dc link voltage is desired. The effects of parameter variation (particularly, stator resistance) on the performance of the direct torque control. It is necessary the addition of parameter adaptation algorithm to compensate this effects. A novel direct torque control of five-phase induction motor using a new switching table combined with an adaptive variable structure observer to avoid the effects of stator resistance variations is presented in this paper. Simulation results provided show the effectiveness of the proposed control strategy.

Keywords Direct torque control · Induction motor · Pulse width modulation · Five-phase motor · Luenberger-sliding mode observer · Voltage source inverter

✉ Atif Iqbal
atif.iqbal@qu.edu.qa

Hamdi Echeikh
echeikh_hamdi@hotmail.com

Ramzi Trabelsi
trabelsi.ramzi@yahoo.fr

Mohamed Faouzi Mimouni
mfaouzi.mimouni@enim.rnu.tn

[1] National Engineering School, Monastir, Tunisia

[2] High Institute of Applied Sciences and Technology, Sousse, Tunisia

[3] Qatar University, Doha, Qatar

1 Introduction

For historical reasons, three-phase machines are widely used: Their design and feeding problems are now well mastered. However, multiphase machines (in which the number of phases is greater than three) have particularly attractive characteristics. First, the increase in the number of phases implies a reduction in the electromagnetic torque ripple. The multiphase machine is, therefore, an interesting solution for demanding applications in terms of vibratory or acoustic discretion. Additionally, a structure with many phases increases the possibilities of operation under fault condition while maintaining an acceptable torque quality (amplitude and ripple). Moreover, an increase in the number of phases implies splitting of power, which reduces the design constraints on the components of power electronics supplying each phase. Therefore, the choice of the multiphase structure sometimes comes from the need in very high power applications.

Practically, multiphase motors are used in the areas of railway traction, naval propulsion, automotive and aerospace. Over the years, many other beneficial features of multiphase machines and drives have become recognized. The pace of research started accelerating in the second half of the 1990s, predominantly due to the developments in electric ship propulsion, which remains nowadays one of the main application areas for multiphase variable-speed drives [1–3]. The types of multiphase machines for variable-speed

Published online: 11 September 2017

applications are in principle the same as their three-phase counterparts. There are induction and synchronous multiphase machines, where a synchronous machine may be with permanent magnet excitation, with field winding, or of reluctance type. Three-phase machines are normally designed with a distributed stator winding that gives near-sinusoidal magnetomotive force (MMF) distribution and is supplied with sinusoidal currents (the exception is the permanent magnet synchronous machine with trapezoidal flux distribution and rectangular stator current supply, known as brushless dc machine, or simply BDCM). Nevertheless, spatial MMF distribution is never perfectly sinusoidal and some spatial harmonics are inevitably present. Multiphase machines show more versatility in this aspect. A stator winding can be designed to yield either near-sinusoidal or quasi-rectangular MMF distribution, by using distributed or concentrated windings, for all ac machine types. Near-sinusoidal MMF distribution requires the use of more than one slot per pole per phase. As the number of phases increases, it becomes progressively difficult to realize a near-sinusoidal MMF distribution. For example, a five-phase four-pole machine requires a minimum of 40 slots for this purpose, while in a seven-phase four-pole machine at least 56 slots are needed. (For a three-phase four-pole machine, the minimum number of slots is only 24.) Multiphase machines where an attempt is made to realize near-sinusoidal MMF distribution by using an appropriate number of slots are termed, henceforth, for simplicity and brevity, machines with sinusoidal MMF. In the literature, one can find several papers presented on modeling and control of multiphase machines [4–14]. The speed control of multiphase electrical machines is similar to three-phase machines.

Constant V/f control is nowadays of relatively little interest, since the cost of implementing more sophisticated control algorithms is negligible compared to the cost of multiphase power electronics and the multiphase machine itself (neither are available on the market).

As long as a symmetrical multiphase machine with sinusoidally distributed stator winding is under consideration, the same vector control schemes as for a three-phase machine are directly applicable regardless of the number of phases. The only difference is that the coordinate transformation has to produce an n-phase set of stator current (or stator voltage) references, depending on whether current control is in the stationary or in the synchronous rotating reference frame. Concerning three-phase machines, one notices the existence of two different approaches for direct torque control. The first is based on the use of a hysteresis stator and torque control in association with an optimum selection table of the stator voltage which leads usually to a variable switching frequency. The second approach is based on applying an adequate PWM control for the inverter (mostly space vector technique). In conclusion, the two DTC approaches are well applicable to multiphase machines. In case of multiphase machines with sinusoidal distributed MMF, the direct torque control scheme requires applying stator sinusoidal voltages to the machine; the research community has proposed different schemes for DTC of multiphase induction machines. In [15], the authors proposed a DTC for five-phase induction motor, to eliminate the common-mode voltages and to reduce the current harmonics. Another method is proposed in [16–19] to improve firstly the torque ripple and secondly the torque response speed by an adequate choice of voltage vectors. Moreover, the authors in [20] developed DTC of five-phase induction motor using duty cycle optimization. The goal of this technique is to reduce the ripple in current and torque, and this is obtained by applying large vectors for each sampling period. A DTC is proposed and experimentally verified in [21] using sensorless adaptive speed observer and a new switching table. Still the torque ripple in DTC is one of the most researched subjects in a large number of research publications. For example in [22], the authors proposed a DTC based on fuzzy logic controller. The reader is referred to [23–27] for more information about the DTC applied for multiphase machines. In summary, DTC offers many advantages such as high dynamic performance even at locked rotor, absence of coordinate transform, absence of voltage modulator block as well as other PID controllers for flux and minimal torque response time even better than the vector controllers. Also, some disadvantages are possible problems during starting, inherent of torque and flux ripples, and the most important drawback is that DTC suffers when there is a parameter variation (especially the stator resistance).

The authors are not aware of any work which tackles control issues arising out of stator resistance variation in multiphase motors. This paper proposes a mechanism of estimation of stator resistance using Luenberger-sliding mode observer for direct torque control of five-phase induction motor using stator current and voltage measurements to compensate the effects of stator resistance variation and new selection table to ameliorate the torque and flux ripple. No additional sensors are used for the proposed scheme.

2 Luenberger-sliding mode observer with stator resistance adaption

Several types of estimation algorithms to develop the identification of the electrical parameters of an induction motor are presented in the literature. Extended Luenberger, extended Kalman filter observers and artificial intelligence are used to observe the rotor flux and the rotor resistance [28–30]. Those methods generally depend upon large memories, extensive computations and large processor time. Thus, a difficult appears with the two observers (extended Kalman filter and extended Luenberger) to achieve and obtain a dynamic response in the existence of errors in estimated

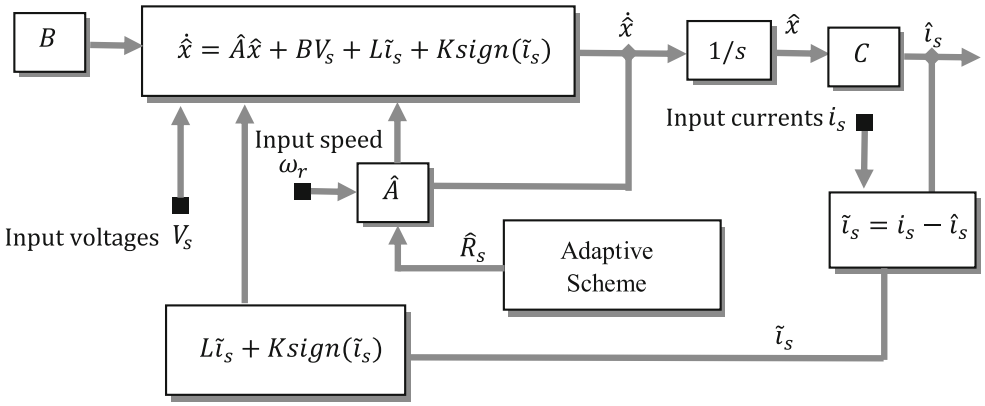

Fig. 1 Luenberger-sliding mode observer structure for stator resistance adaption

quantities [31]. An observer has been developed to estimate the most critical parameters by giving an adequate motor model [32,33]. Model reference adaptive systems (MRAS) deliver correct estimation, but they converge quite slowly [33]. However, exact knowledge of the motor parameter is not a certainty which makes it difficult for these observers to work in internal noise or large disturbances in the system. Jansen and Lorenz [34] developed general design and parameters sensitivity in both open-loop and closed-loop observers with speed estimation using the deterministic Luenberger observer. Indeed, a better performance obtained in closed loop with a feedback adjustment. Further, the robustness and accuracy of the observer in closed loop depends on the accuracy of the measured variables. Closed-loop observers for direct field-oriented induction machine drive also show satisfactory performance in a wide operating speed range including zero and field weakening region [35]. In this paper, the observer presented has acceptable robustness and is insensitive to the existence of measurement noise and disturbance. This paper presented a novel Luenberger-sliding mode observer applied for DTC control of five-phase induction motor with an adaption method for the stator resistance variation. The observer is a sixth-order observer and offers significantly fewer computation problems compared to the observers proposed in the literature. In addition, the sliding mode gains are easy to set and the gains of Luenberger part of the observer obtained using the five-phase motor model. Moreover, combing the sliding mode observer with the Luenberger part enables quick tracking of the flux and the parameters. Furthermore, the Luenberger part is sufficient and the sliding mode part takes care of the internal noise, significant mismatches and the large disturbances on the measurement. Figure 1 shows detailed block diagram of the presented Luenberger-sliding mode observer.

The five-phase induction motor model is given in state equations as follows:

$$\begin{aligned} \dot{x} &= \boldsymbol{A}x + \boldsymbol{B}V_s \\ i_s &= \boldsymbol{C}x \end{aligned} \tag{1}$$

where $x = \begin{bmatrix} i_s & \emptyset_s \end{bmatrix}^{\mathrm{T}}$, $i_s = \begin{bmatrix} i_{s\alpha} & i_{s\beta} & i_{sx} & i_{sy} \end{bmatrix}^{\mathrm{T}}$, $\emptyset_s = \begin{bmatrix} \emptyset_{s\alpha} & \emptyset_{s\beta} \end{bmatrix}^{\mathrm{T}}$.

$$A = \begin{bmatrix} -\left(\frac{R_s}{\sigma L_s} + \frac{R_r}{\sigma L_r}\right)\boldsymbol{I} + \omega_r \boldsymbol{J} & \boldsymbol{0} & \frac{R_r}{\sigma L_r L_s}\boldsymbol{I} - \frac{\omega_r}{\sigma L_s}\boldsymbol{J} \\ \boldsymbol{0} & -\frac{1}{\tau_{ls}}\boldsymbol{I} & \boldsymbol{0} \\ -R_s\boldsymbol{I} & \boldsymbol{0} & \boldsymbol{0} \end{bmatrix} \tag{2}$$

$$\boldsymbol{B} = \begin{bmatrix} \frac{1}{\sigma L_s}\boldsymbol{I} & \boldsymbol{0} \\ \boldsymbol{0} & \frac{1}{L_{ls}}\boldsymbol{I} \\ \boldsymbol{H} & \boldsymbol{G} \end{bmatrix} \tag{3}$$

$$C = \begin{bmatrix} \boldsymbol{I} & \boldsymbol{0} & \boldsymbol{0} \\ \boldsymbol{0} & \boldsymbol{I} & \boldsymbol{0} \end{bmatrix} \tag{4}$$

The matrixes ***I, J, H*** and ***G*** are given by the following expressions gives, respectively, as:

$$\boldsymbol{I} = \begin{bmatrix} 1 & 0 \\ 0 & 1 \end{bmatrix}, \boldsymbol{J} = \begin{bmatrix} 0 & -1 \\ 1 & 0 \end{bmatrix}, \boldsymbol{H} = \begin{bmatrix} 0 & 1 \\ 0 & 0 \end{bmatrix}, \boldsymbol{G} = \begin{bmatrix} 0 & 0 \\ 1 & 0 \end{bmatrix} \tag{5}$$

$\sigma = 1 - L_m^2/L_s L_r$, $\tau_{ls} = L_{ls}/R_s$ and i_s, V_s, $\emptyset_s$ are, respectively, the stator currents, voltages and flux in the reference frames $(\alpha\beta)$ and (xy). L_s, L_r, R_s, R_r, L_{ls}, L_m and L_{lr} denotes, respectively, the stator inductance, rotor inductance, stator resistance, rotor resistance, stator leakage inductance, magnetizing inductance and rotor leakage inductance. The proposed Luenberger-sliding mode observer to estimate simultaneously the stator current, stator flux and the stator resistance is given by

$$\begin{aligned} \dot{\hat{x}} &= \hat{\boldsymbol{A}}\hat{x} + \boldsymbol{B}V_s + \overbrace{\boldsymbol{L}\tilde{i}_s}^{\substack{\textbf{\textit{Luenberger}} \\ \textbf{\textit{observer}} \\ \textbf{\textit{part}}}} + \overbrace{\boldsymbol{K}\mathrm{sign}(\tilde{i}_s)}^{\substack{\textbf{\textit{Sliding mode}} \\ \textbf{\textit{observer}} \\ \textbf{\textit{part}}}} \\ \hat{i}_s &= \boldsymbol{C}\hat{x} \end{aligned} \tag{6}$$

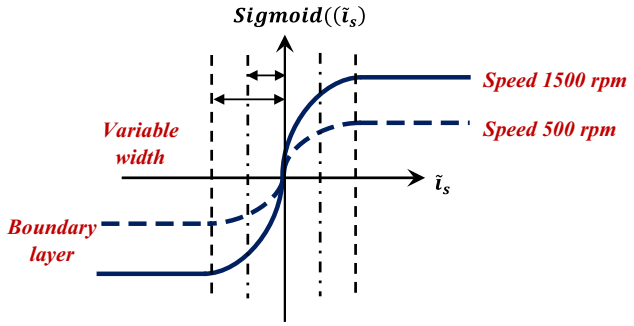

Fig. 2 Variable boundary layers per the speed

The sliding mode observer (SMO) is robust against the parameter variations and external disturbances. The quality of the characteristic is governing the parameter variation and external disturbance via the action of the discontinuous (signum). SMO is well known for chattering problem due to the use of the signum function as switching function; however, to solve this problem a sigmoid function is applied as a switching function represented by the expression in equation (5).

$$\text{Sigmoid}((\tilde{i}_s) = \left(\frac{2}{1+\mathrm{e}^{-a\tilde{i}_s}}\right) - 1 \tag{7}$$

where a is a positive constant and has the role to regulate the slope of the sigmoid function.

The signum functions are either -1 or 1, while the sigmoid functions are presented in a certain range given by $-1 < \text{Sigmoid}((\tilde{i}_s) < 1$. The Lyapunov stability condition is satisfied by the multiplication of the sigmoid functions by an adequate gain $\boldsymbol{K}$. Taking into consideration this approximation, equation (5) can be rewritten as

$$\begin{aligned}\dot{\hat{x}} &= \hat{\boldsymbol{A}}\hat{x} + \boldsymbol{B}V_s + \overbrace{\boldsymbol{L}\tilde{i}_s}^{\textit{Luenberger observer part}} + \overbrace{\boldsymbol{K}\left(\left(\frac{2}{1+\mathrm{e}^{-a\tilde{i}_s}}\right) - 1\right)}^{\textit{Sliding mode observer part}} \\ \hat{i}_s &= \boldsymbol{C}\hat{x}\end{aligned} \tag{8}$$

Keeping the switching frequency constant, in an electric angle period, the number of switches is reduced for high speed compared to the low speed. Therefore, it is mandatory to adjust the observer gains according to switch delays [36]. Moreover, any variation in the rotational speed is in accord with a change in the boundary layer as shown in Fig. 2. When the number of the revolutions per minute increases, the width of the boundary layer changes and becomes large to guarantee the response time for the switching. Furthermore, a large chattering appears at a high speed with a rise of the response time when the width is kept constant as compared to the speed per minute.

Stability analysis of the proposed method

To design the gains L and K taking into account that the limit of time $t \to \infty$ of $\hat{x} - x \to 0$ and $\hat{i}_s - i_s \to 0$. Thus, the output dynamics errors can be written by subtracting equation (6) from equation (1).

$$\begin{aligned}\frac{\mathrm{d}S_{\alpha\beta}}{\mathrm{d}t} &= \boldsymbol{C}\frac{\mathrm{d}(x-\hat{x})}{\mathrm{d}t} = \boldsymbol{C}(\boldsymbol{A}-\boldsymbol{LC})\boldsymbol{C}^{\mathrm{T}}S_{\alpha\beta} \\ &\quad - \boldsymbol{C}\tilde{\boldsymbol{A}}\hat{x} - \boldsymbol{CK}\left(\left(\frac{2}{1+\mathrm{e}^{-aS_{\alpha\beta}}}\right) - 1\right)\end{aligned} \tag{9}$$

where $\tilde{\boldsymbol{A}} = \hat{\boldsymbol{A}} - \boldsymbol{A}$.

The error in the steady state becomes quite large at low speed; therefore, the adjustment in gain K is required with the rotational speed as $K_{\text{ad}} = K\omega_{\text{ref}}$ and the ω_{ref} is heuristically determined.

To determine the error dynamics, Lyapunov's stability criterion is used, which gives sufficient condition for asymptotic stability of a nonlinear system. The following Lyapunov's function is introduced to derive an expression for stator resistance estimation:

$$V_{\alpha\beta} = S_{\alpha\beta}^{\mathrm{T}}S_{\alpha\beta} + \frac{\left(\hat{R}_s - R_s\right)^2}{G} \tag{10}$$

where G is a positive constant.

Using the expression of the dynamics of the errors given in Eq. (7), the derivative of $V_{\alpha\beta}$ becomes

$$\begin{aligned}\dot{V}_{\alpha\beta} &= \Big[S_{\alpha\beta}^{\mathrm{T}}[\{\boldsymbol{C}(\boldsymbol{A}-\boldsymbol{LC})\boldsymbol{C}^{\mathrm{T}}\}^{\mathrm{T}} + \{\boldsymbol{C}(\boldsymbol{A}-\boldsymbol{LC})\boldsymbol{C}^{\mathrm{T}}\}S_{\alpha\beta}] \\ &\quad - \boldsymbol{K}^{\mathrm{T}}\boldsymbol{C}^{\mathrm{T}}S_{\alpha\beta}\left(\left(\frac{2}{1+\mathrm{e}^{-aS_{\alpha\beta}}}\right) - 1\right) \\ &\quad - S_{\alpha\beta}^{\mathrm{T}}\boldsymbol{CK}\left(\left(\frac{2}{1+\mathrm{e}^{-aS_{\alpha\beta}}}\right) - 1\right)\Big] \\ &\quad - 2\boldsymbol{C}\hat{\boldsymbol{A}}\hat{x}S_{\alpha\beta} + \frac{2\left(\hat{R}_s - R_s\right)}{G}\dot{\hat{R}}_s\end{aligned} \tag{11}$$

The term $\frac{(\hat{R}_s - R_s)^2}{G}$ is a variable parameter and it is used to obtain an estimation of the stator resistance. To verify the Lyapunov stability approach, the sliding mode state can be derived satisfying the condition of Lyapunov that $V_{\alpha\beta} > 0$ and $\dot{V}_{\alpha\beta} < 0$. The derivative of Lyapunov function $\dot{V}_{\alpha\beta}$ is definite negative since the first term of Eq. (9) is constantly negative. Thus, the stability condition is satisfied by choosing the second term of Eq. (9) to be zero.

$$\begin{cases} \left[\begin{array}{c} S_{\alpha\beta}^{\mathrm{T}}[\{\boldsymbol{C}(\boldsymbol{A}-\boldsymbol{LC})\boldsymbol{C}^{\mathrm{T}}\}^{\mathrm{T}}+\{\boldsymbol{C}(\boldsymbol{A}-\boldsymbol{LC})\boldsymbol{C}^{\mathrm{T}}\}S_{\alpha\beta}]-\boldsymbol{K}^{\mathrm{T}}\boldsymbol{C}^{\mathrm{T}}S_{\alpha\beta}\left(\left(\frac{2}{1+\mathrm{e}^{-aS_{\alpha\beta}}}\right)-1\right) \\ -S_{\alpha\beta}^{\mathrm{T}}\boldsymbol{CK}\left(\left(\frac{2}{1+\mathrm{e}^{-aS_{\alpha\beta}}}\right)-1\right)<0 \end{array} \right] \\ -2\boldsymbol{C}\hat{\boldsymbol{A}}\hat{x}S_{\alpha\beta}+\frac{2(\hat{R}_s-R_s)}{G}\dot{\hat{R}}_s=0 \end{cases} \tag{12}$$

To obtain the equation describing the estimation of the stator resistance, one needs to develop the second part of Eq. (10).

$$\dot{\hat{R}}_s=\frac{G}{\sigma L_s}(S_\alpha\hat{\imath}_{s\alpha}+S_\beta\hat{\imath}_{s\beta}) \tag{13}$$

where $S_\alpha=i_{s\alpha}-\hat{\imath}_{s\alpha}$ and $S_\beta=i_{s\beta}-\hat{\imath}_{s\beta}$.

3 Direct torque control of five-phase induction motor

The direct torque control (DTC) offers direct control of the torque and stator flux. However, this method offers a methodical solution to improve the operation characteristics of both the motor and the voltage source inverter (VSI). Direct torque control allows achievement of an effective and rapid control of the torque and stator flux by using an optimal selection of the inverter switching states. This issue becomes complex in case of multiphase machines because the additional switches of the inverter allow larger flexibility in their selection, which offer a great adjustment of the torque and flux. On the other hand, for the three-phase motor the control implemented using only limited inverter switches (eight possible). More selection criteria are presented due to the large number of the inverter switches. Due to this reason, little research has been done on the switching table selection for the DTC of multiphase motor drives. DTC of five-phase induction machines has been reported in [4]; nevertheless, there are no criteria presented to select the inverter states. In the literature, one finds different switching tables for the DTC, some of which are discussed in [8,13] with high performance of flux and torque regulation, but does not solve the current ripple problems. So, research is required for switching table selection for multiphase motor drives such as in [13]. However, in [37] a selection criterion has been proposed for five-phase permanent magnet motors, but this control technique has two drawbacks: The low-frequency ripple was not eliminated and dc link voltage is not fully utilized. In this paper, a novel direct torque control has been proposed with two features: first, the elimination of the harmonic currents with low-frequency and torque ripple improvement and, second, stator resistance estimation of direct torque control to avoid the effects of the stator resistance of five-phase induction motor at low speed. The proposed direct torque controller relates to the adaptive Luenberger-sliding mode observer. The resulting control scheme is verified with simulation. There are 32 possible switching states for the five-leg inverter associated with a five-phase induction motor. The inverter switching number is defined in binary as $[G_a, G_b, G_c, G_d, G_e]$, where the G_a–G_e denote the gate signal to the upper switches; for more explanation, refer to Fig. 3.

Moreover, the five-phase voltages of the inverter are transformed into two different voltage vectors using the transformation given in Eq. (11). Therefore, the two-voltage vectors are presented in their associated $(\alpha-\beta)$ and $(x-y)$ spaces. However, repeating the aforesaid process for all 32 inverter states, the two inverter planes are formulated as shown in Fig. 4. It is clear that each plane contains three concentric decagons with different magnitudes such as $(\sqrt{5}-1)V_{\mathrm{dc}}/5$, $2V_{\mathrm{dc}}/5$ and $(\sqrt{5}+1)V_{\mathrm{dc}}/5$. The constant $(\sqrt{5}-1)/2$ considers the ratio between two successive magnitudes. The voltages vectors are classified into four different groups according to the magnitudes (null, small, medium, large).

According to the five-phase drive switching states, there are different possible load configurations. In addition, those configurations are depending on the number of the windings connected to either the negative or the positive rail of the voltage source inverter, namely those configurations 5–0, 4–1, 3–2, 2–3, 1–4 and 0–5. From Fig. 4, one can summarize the following properties.

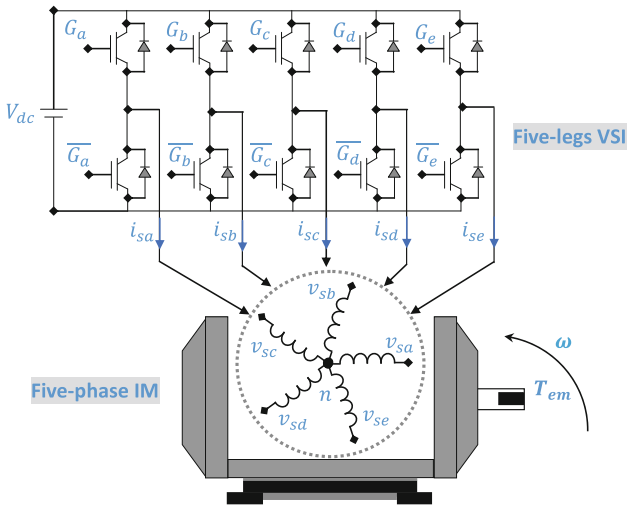

Fig. 3 Five-phase drive system (motor and inverter)

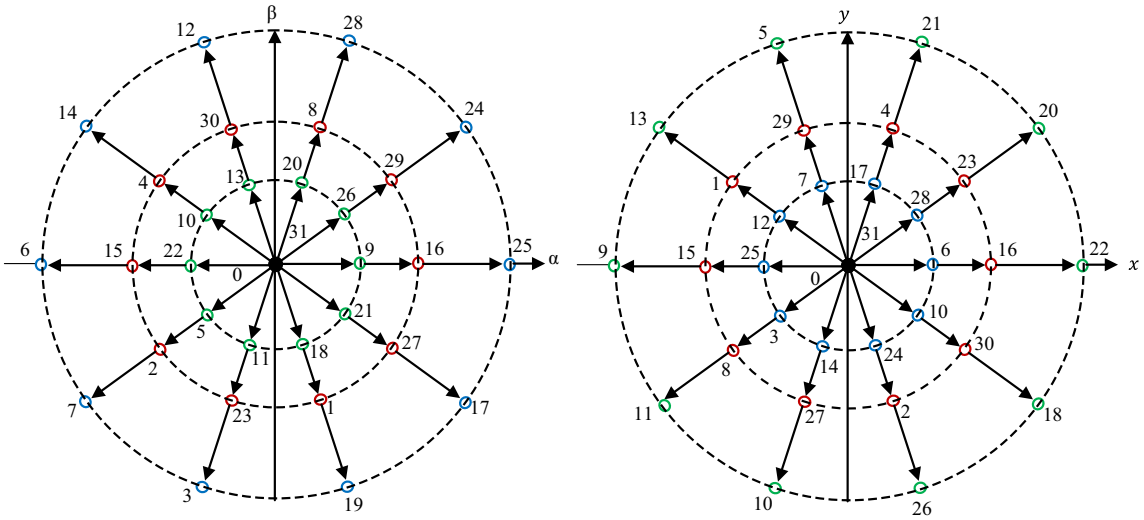

Fig. 4 Vectors for a five-phase inverter in $(\alpha - \beta)$ and $(x - y)$ planes

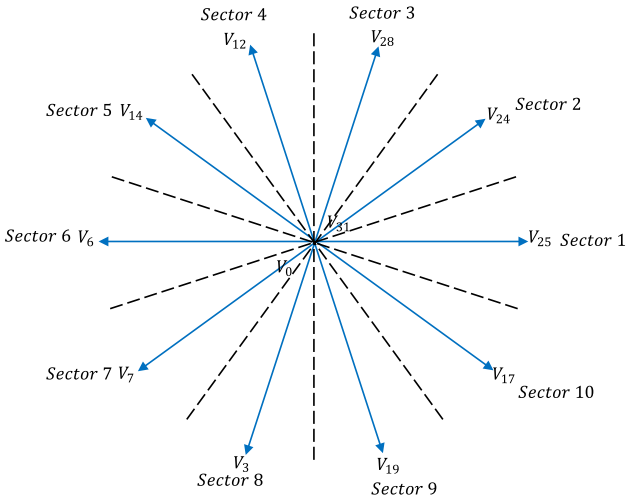

Fig. 5 Active voltage vectors and sectors in the $(\alpha - \beta)$ plane

- The configuration $\{0-5, 5-0\}$ allows the production of the null voltage vector in both planes $(\alpha-\beta)$ and $(x-y)$ and the inverter state $(0, 0, 0, 0, 0)$.
- The configuration $\{4-1, 1-4\}$ allows the production of the medium voltage vector in both planes $(\alpha-\beta)$ and $(x-y)$, the inverter state $(1, 1, 1, 0, 1)$ and the vector V_{29}.

The configuration $\{3-2, 2-3\}$ allows the production of the large voltage vector in the $(\alpha - \beta)$ plane and small vector in the plane $(x - y)$, the inverter state $(1, 1, 0, 0, 1)$ and the vector V_{25}, or one small voltage vector in the $(\alpha - \beta)$ plane and one large the $(x-y)$ plane, the inverter state $(0, 1, 0, 0, 1)$ and the vector V_9.

As shown in Fig. 4, the two-aligned large and medium voltage vectors in the plane $(\alpha - \beta)$ given by the vectors

Table 1 Voltage vectors for the proposed direct torque controller

$\Delta\emptyset$	ΔT_e	Sector number									
		1	2	3	4	5	6	7	8	9	10
+1	+1	V_{24}	V_{28}	V_{12}	V_{14}	V_6	V_7	V_3	V_{19}	V_{17}	V_{25}
	−1	V_{17}	V_{25}	V_{24}	V_{28}	V_{12}	V_{14}	V_6	V_7	V_3	V_{19}
−1	+1	V_{14}	V_6	V_7	V_3	V_{19}	V_{17}	V_{25}	V_{24}	V_{28}	V_{12}
	−1	V_7	V_3	V_{19}	V_{17}	V_{25}	V_{24}	V_{28}	V_{12}	V_{14}	V_6
+1	0	V_0	V_{31}	V_0	V_{31}	V_0	V_{31}	V_0	V_{31}	V_0	V_{31}
−1	0	V_{31}	V_0	V_{31}	V_0	V_{31}	V_0	V_{31}	V_0	V_{31}	V_0

16 and 25 produce small and medium vectors with opposite directions in the $(x - y)$ plane. Ten active vectors and two null vectors will be used in the selection table of the direct torque controller as shown in Fig. 5.

There are ten active voltage vectors and two null vectors (V_{31} and V_0) only used to the direct torque controller. The concept is very important, and only the $(\alpha - \beta)$ plane is used to produce the torque and flux. In the case of the stator flux-oriented control, the control of flux is based in d-component of the stator voltage and the q-component is used to control the torque. The selection of the correct inverter states based on the position of the d-axis of the stator flux linkage in the $(\alpha - \beta)$ plane. However, to obtain information about the position of the stator flux linkage requires a definition of the sector. Based on the torque and flux errors, adequate inverter states should be used. In this case, flux (two-level) and torque (three-level) hysteresis comparators are used. As an example, in sector 1, when the motor is running precisely in low-speed region, only two active voltages and two null will be used to adjust the torque and flux, and the selection of the voltage vector criterion is presented as follows: If the torque and flux

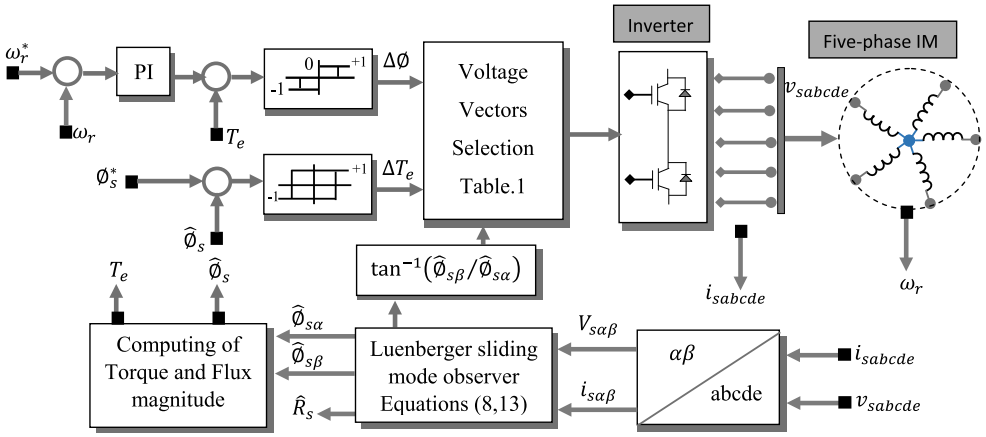

Fig. 6 Block diagram of adaptive direct torque control of a five-phase induction motor drive

Table 2 Five-phase induction motor data

Symbols	Quantity	Value
R_r	Rotor resistance	6.3 Ω
R_s	Stator resistance	10 Ω
L_r	Rotor inductance	0.46 H
L_s	Stator inductance	0.46 H
L_{ls}	Stator leakage inductance	0.04 H
L_{lr}	Rotor leakage inductance	0.04 H
M	Mutual inductance	0.42 H
J	Inertia moment	0.01
P	Pair of pole	2
$\emptyset_{sn}$	Rated flux	1.2705 wb
T_{en}	Rated torque	8.33 Nm
N	Rated speed	1500 rpm

must be increased $\Delta\emptyset = +1$ and $\Delta T_e = +1$, the vector is selected (V_{24}). If the torque must be decreased and flux must be increased $\Delta\emptyset = +1$ and $\Delta T_e = -1$, the active voltage V_{17} is selected. If the torque is to be increased and the flux is to be decreased $\Delta\emptyset = -1$ and $\Delta T_e = +1$, the vector V_{14} is selected. If both the torque and flux are to be decreased $\Delta\emptyset = -1$ and $\Delta T_e = -1$, the vector V_7 is selected. And if the torque error $\Delta T_e = 0$, the vector null V_0 or V_{31} is selected regardless of the vector V_7 being selected. And if the torque error $\Delta T_e = 0$, the vector null V_0 or V_{31} is selected regardless of the output of the flux control loop; Table 1 summarizes the voltage vectors table for proposed direct torque controller.

4 System synthesis and simulation results

Figure 6 illustrates the block diagram of the direct torque control of five-phase system. The system consists of four basic functions, which are designed as follows: The five-phase IM model, estimations of the stator flux and torque, Luenberger-sliding mode observer to obtain the stator resistance equation, two- and three-level hysteresis controllers where the flux magnitude and torque references are compared with both quantities calculated from the five-phase IM and finally the suitable switching states which converts the controller outputs into suitable commands to the power electronic switching devices.

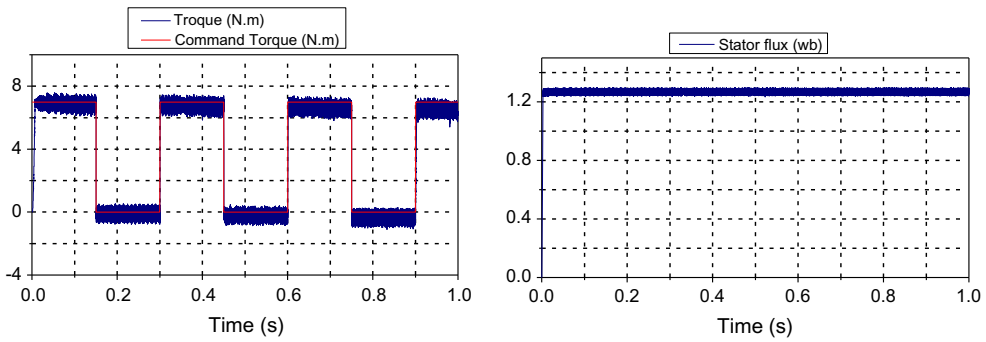

Fig. 7 Case 1 torque and magnitude flux

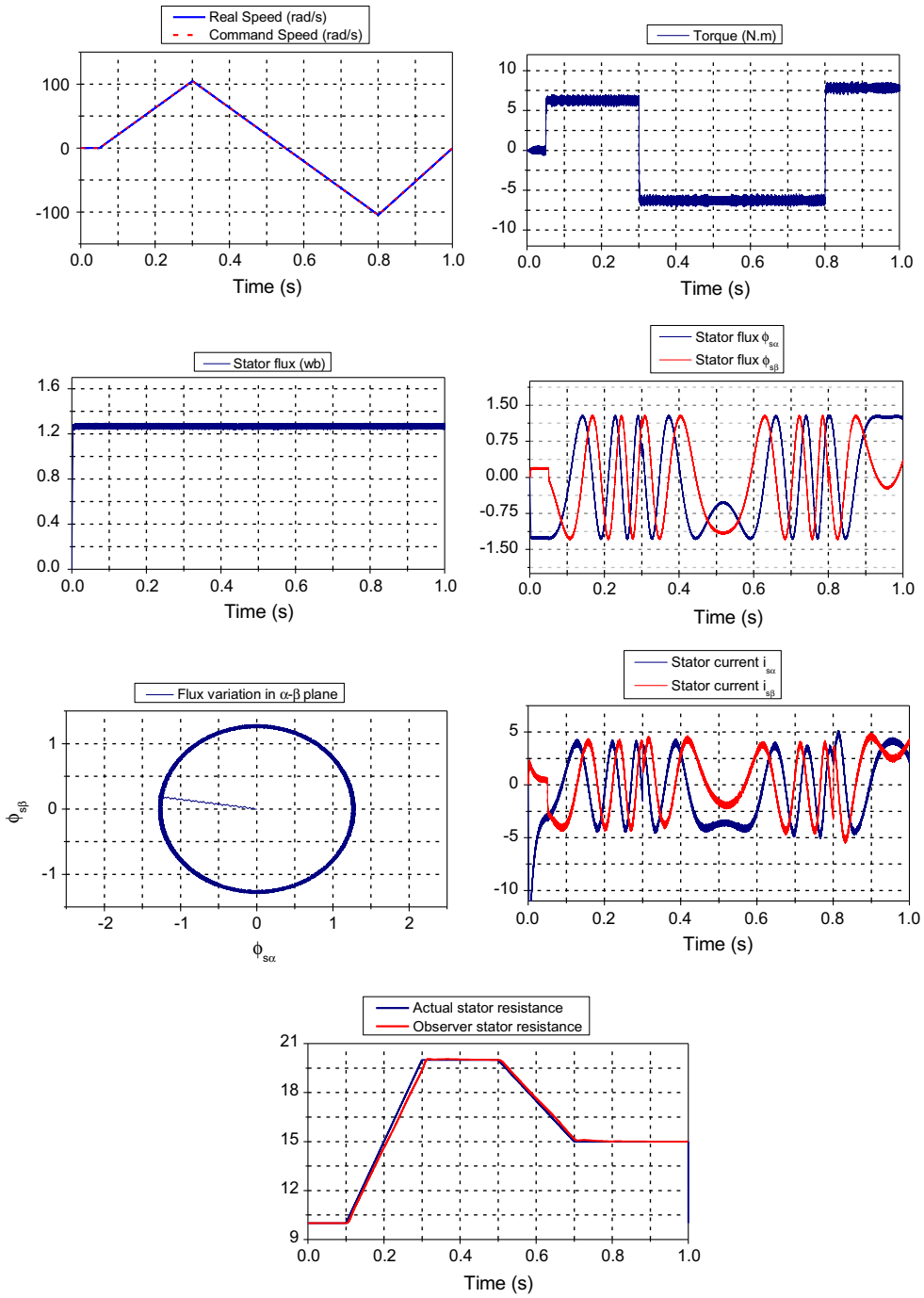

Fig. 8 Case 2 triangular reference speed and no load

The simulation of the DTC algorithm with stator resistance adaptation has been conducted for the 1.5kW 230V four-pole five-phase induction machine; the motor data are presented in Table 2. Simulation has been adapted for various cases without and with a speed loop. Figure 7 shows the torque response of the five-phase IM to frequent step change in the command torque of 6 Nm. Figure 8 shows the simulation results under triangular reference speed and no load. Figure 9 presents the simulation results under reference speed ramp up, reaches the steady state of 100 rad/s, slows down and reverses the direction of rotation under load. In Fig. 7, only the electromagnetic torque and flux magnitude are presented, and for both Figs. 8 and 9, respectively, the speed, torque, magnitude of flux, the stator fluxes $\emptyset_{s\alpha}$, $\emptyset_{s\beta}$, the flux evolution in the reference plane $(\alpha - \beta)$, the stator currents $i_{s\alpha}$, $i_{s\beta}$ and the observed stator resistance are illustrated.

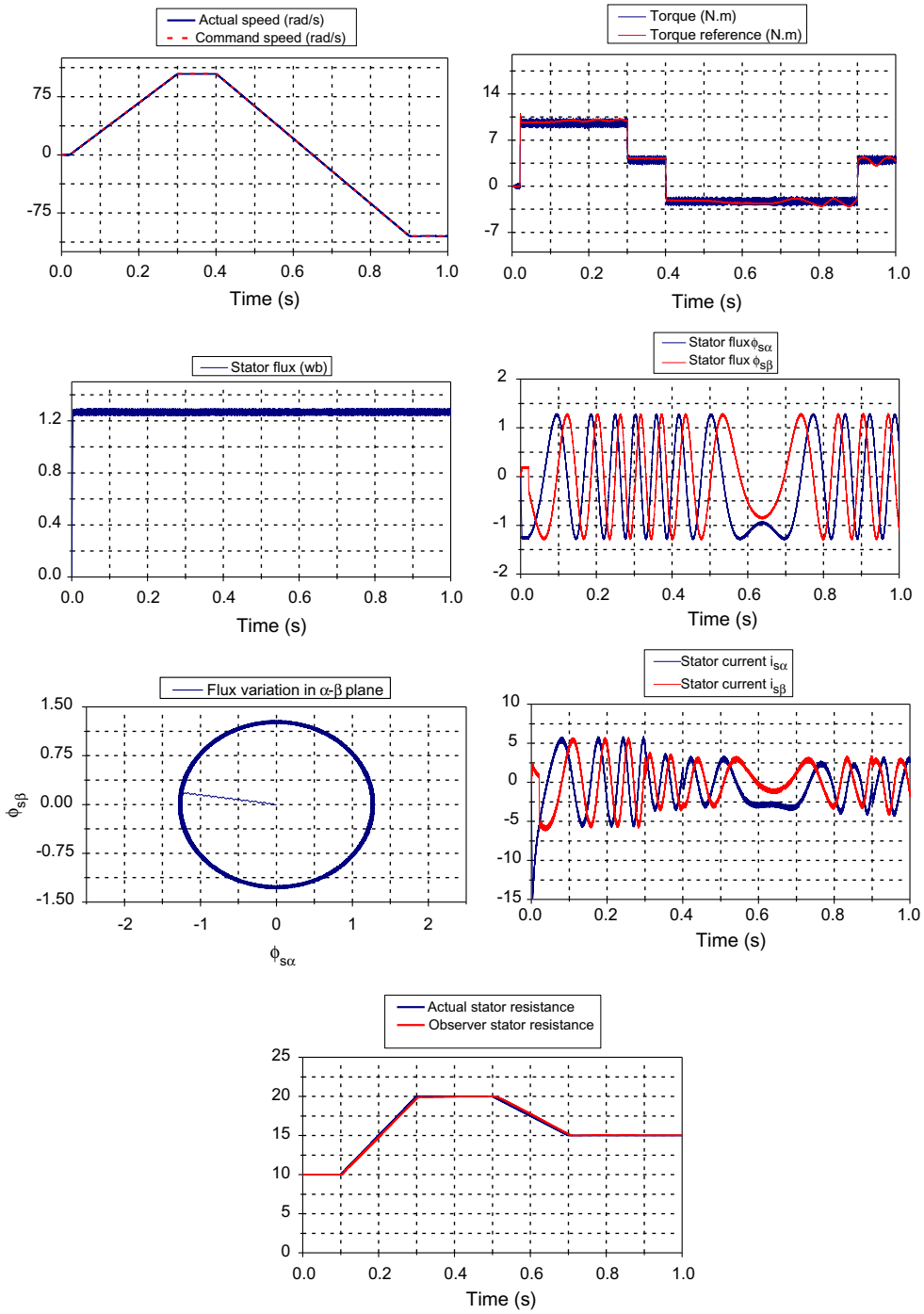

Fig. 9 Case 3 trapezoidal reference and with load

One can understand that the direct torque control of five-phase IM provides fast response for the torque and speed under reversing operation, and also it is clearly shown that the stator flux follows its reference and is assumed that the trajectory of the stator flux in the reference frame is circular.

The estimated stator resistance is fed back to the controller, since it is the most critical parameter in the controller algorithm that changes due to temperature, skin effect or other no idealities. Temperature has the most dominant effect on rotor resistance as well as on stator resistance. Rotor resistance can change from ambient temperature values to hot (up to maximum operating temperature) values by about 20–100%. The simulations results have been carried out for increase of 100% of the stator resistance in the motor model. The simulations show simultaneously the performance of the novel Luenberger-sliding mode observer for the estimation of the

stator resistance using the adaption law. Moreover, the key to stator resistance adaptation is to correct the flux $\emptyset_s$ and to avoid all the effects due to its variations.

5 Conclusion

In this paper, the mathematical model of the five-phase induction motor is developed in the rotating reference frames, and then an observer based on the Luenberger-sliding mode has been governing in order to estimate simultaneously the stator flux and the stator resistance to avoid all the effects of the stator resistance variation due to the temperature. Finally, the DTC of the five-phase IM has been developed based on the derived model and control strategy, based on 32 voltage vectors which offer, in the case of multiphase motor, more flexibility. The proposed method has been verified using various cases which shows high performances. Moreover, the DTC still has problems such as high current and torque ripple due to the variable switching frequency and high noise level at low speed. In our future work, one use new DTC based on nonlinear approach based on Lyapunov's stability (constant switching frequency) to avoid these problems.

References

1. Ferreira CL, Bucknall RWG (2004) Modelling and real-time simulation of an advanced marine full-electrical propulsion system. In: Second international conference on power electronics, machines and drives (PEMD 2004), vol 2, pp 574–579
2. Terrien F, Siala S, Noy P (2004) Multiphase induction motor sensorless control for electric ship propulsion. In: Second international conference on power electronics, machines and drives (PEMD 2004), vol 2, pp 556–561
3. Smith S (2002) Developments in power electronics, machines and drives. Power Eng J 16(1):13–17
4. Xu H, Toliyat HA, Petersen LJ (2002) Five-phase induction motor drives with DSP-based control system. IEEE Trans Power Electron 17(4):524–533
5. Parsa L, Toliyat HA (2005) Five-phase permanent-magnet motor drives. IEEE Trans Ind Appl 41(1):30–37
6. Lyra ROC, Lipo TA (2002) Torque density improvement in a six-phase induction motor with third harmonic current injection. IEEE Trans Ind Appl 38(5):1351–1360
7. Kianinezhad R, Nahid B, Betin F, Capolino GA (2004) A new field orientation control of dual three phase induction machines. In: 2004 IEEE international conference on industrial technology, 2004. IEEE ICIT '04, vol 1, pp 187–192
8. Hatua K, Ranganathan VT (2005) Direct torque control schemes for split-phase induction machine. IEEE Trans Ind Appl 41(5):1243–1254
9. De Camillis L, Matuonto M, Monti A, Vignati A (2001) Optimizing current control performance in double winding asynchronous motors in large power inverter drives. IEEE Trans Power Electron 16(5):676–685
10. Bojoi R, Profumo F, Tenconi A (2003) Digital synchronous frame current regulation for dual three-phase induction motor drives. In: Power electronics specialist conference, 2003. PESC '03. 2003 IEEE 34th annual, vol 3, pp 1475–1480
11. Bojoi R, Lazzari M, Profumo F, Tenconi A (2003) Digital field-oriented control for dual three-phase induction motor drives. IEEE Trans Ind Appl 39(3):752–760
12. Bojoi R, Farina F, Tenconi A, Profumi F, Levi E (2006) Dual three-phase induction motor drive with digital current control in the stationary reference frame. Power Eng 20(3):40–43
13. Bojoi R, Farina F, Griva G, Profumo F, Tenconi A (2005) Direct torque control for dual three-phase induction motor drives. IEEE Trans Ind Appl 41(6):1627–1636
14. Klingshirn EA (1983) High phase order induction motors—part I. Description and theoretical considerations. IEEE Power Eng Rev PER–3(1):27
15. Tatte YN, Member S, Aware MV (2016) Direct torque control of five-phase induction motor with common-mode voltage and current harmonics reduction. IEEE Trans Power Electron 8993(c):1–11
16. Tatte YN, Aware MV (2014) Torque ripple reduction in five-phase direct torque controlled induction motor. In: 2014 IEEE international conference on power electronics, drives and energy systems (PEDES), pp 1–5
17. Tatte YN (2015) Torque ripple minimization in five-phase three-level inverter fed direct torque control induction motor drive. In: 2015 17th European conference on power electronics and applications (EPE'15 ECCE-Europe), pp 1–6
18. Dhiman S, Hussain A, Kumar V (2016) An effective voltage switching state algorithm for direct torque controlled five-phase induction motor drive to reduce torque ripple. In: 2016 IEEE students' conference on electrical, electronics and computer science (SCEECS), pp 1–6
19. Kang S-Y, Lee K-B (2016) Improved switching selection for direct torque control of a five-phase induction motor. In: 2016 IEEE transportation electrification conference and expo, Asia-Pacific (ITEC Asia-Pacific), pp 651–655
20. Wang T, Yang J (2014) A direct torque control strategy of five-phase induction motor with duty cycle optimization. In: 2014 17th international conference on electrical machines and systems (ICEMS), pp 118–122
21. Zheng L-B, Fletcher JE, Williams BW, He X-N (2011) A novel direct torque control scheme for a sensorless five-phase induction motor drive. IEEE Trans Ind Electron 58(2):503–513
22. Kang S-Y, Shin H-U, Lee KB (2016) Improved torque ripple reduction method of five-phase induction motor using fuzzy controller. In: 2016 IEEE 8th international power electronics and motion control conference (IPEMC-ECCE Asia), pp 635–640
23. Riveros JA, Barrero F, Levi E, Durán MJ, Toral S, Jones M (2013) Variable-speed five-phase induction motor drive based on predictive torque control. IEEE Trans Ind Electron 60(8):2957–2968
24. Vafaie MH, Dehkordi BM, Moallem P, Kiyoumarsi A (2016) A new predictive direct torque control method for improving both steady-state and transient-state operations of the PMSM. IEEE Trans Power Electron 31(5):3738–3753
25. Khaldi BS, Abu-Rub H, Iqbal A, Kennel R, Mahmoudi MO, Boukhetala D (2011) Sensorless direct torque control of five-phase induction motor drives. In: IECON 2011 - 37th annual conference of the IEEE industrial electronics society, pp 3501–3506
26. Riveros JA, Durán MJ, Barrero F, Toral S (2012) Direct torque control for five-phase induction motor drives with reduced common-mode voltage. In: IECON 2012 - 38th annual conference on IEEE industrial electronics society, pp 3616–3621
27. Tabrizchi AM, Soltani J, Shishehgar J, Abjadi NR (2014) Direct torque control of speed sensorless five-phase IPMSM based on adaptive input-output feedback linearization. In: The 5th annual international power electronics, drive systems and technologies conference (PEDSTC 2014), pp 43–48

28. Karanayil B, Rahman MF, Grantham C (2003) Implementation of an on-line resistance estimation using artificial neural networks for vector controlled induction motor drive. In: Industrial Electronics Society, 2003. IECON '03. The 29th annual conference of the IEEE, vol 2, pp 1703–1708
29. Guo L (1990) Estimating time-varying parameters by the Kalman filter based algorithm: stability and convergence. IEEE Trans Autom Control 35(2):141–147
30. Cirrincione M, Pucci M, Cirrincione G, Capolino GA (2003) A new experimental application of least-squares techniques for the estimation of the induction motor parameters. IEEE Trans Ind Appl 39(5):1247–1256
31. Attaianese C, Tomasso G, Damiano A, Marongiu I, Perfetto A (1999) A novel approach to speed and parameters estimation in induction motor drives. IEEE Trans Energy Convers 14(4):939–945
32. Kubota H, Matsuse K (1993) Speed sensorless field oriented control of induction motor with rotor resistance adaptation. In: Conference record of the 1993 IEEE industry applications conference twenty-eighth IAS annual meeting, vol 1, pp 414–418
33. Ohnishi K, Ueda Y, Miyachi K (1986) Model reference adaptive system against rotor resistance variation in induction motor drive. IEEE Trans Ind Electron IE–33(3):217–223
34. Jansen PL, Lorenz RD (1994) A physically insightful approach to the design and accuracy assessment of flux observers for field oriented induction machine drives. IEEE Trans Ind Appl 30(1):101–110
35. Jansen PL, Lorenz RD, Novotny DW (1993) Observer-based direct field orientation: analysis and comparison of alternative methods. In: Conference record of the 1993 IEEE industry applications conference twenty-eighth IAS annual meeting, vol 1, pp 536–543
36. Kim YS, Ryu SL, Kwon YA (2004) An improved sliding mode observer of sensorless permanent magnet synchronous motor. In: SICE 2004 annual conference, vol 1, pp 192–197
37. Parsa L, Toliyat HA (2007) Sensorless direct torque control of five-phase interior permanent-magnet motor drives. IEEE Trans Ind Appl 43(4):952–959